Iron induces protection and necrosis in cultured cardiomyocytes: Role of reactive oxygen species and nitric oxide

Juan Pablo Munoz [a,*], Mario Chiong [a,b], Lorena García [a,b], Rodrigo Troncoso [a,b], Barbra Toro [a,b], Zully Pedrozo [a,b], Jessica Diaz-Elizondo [a,b], Daniela Salas [a,b], Valentina Parra [a,b], Marco T. Núñez [c], Cecilia Hidalgo [a,d], Sergio Lavandero [a,b,d,*]

[a] Centro FONDAP de Estudios Moleculares de la Célula
[b] Departamento de Bioquímica y Biología Molecular, Facultad Ciencias Químicas y Farmacéuticas
[c] Instituto Milenio de Dinámica Molecular y Biotecnología; Facultad de Ciencias, Universidad de Chile, Santiago 838-0492, Chile
[d] Instituto de Ciencias Biomédicas, Facultad de Medicina

ARTICLE INFO

Keywords:
Iron
Nitric oxide
Cell death
Necrosis
Hypertrophy
Cardioprotection
Reactive oxygen species
Cardiomyocyte
Free radicals

ABSTRACT

We investigate here the role of reactive oxygen species and nitric oxide in iron-induced cardiomyocyte hypertrophy or cell death. Cultured rat cardiomyocytes incubated with 20 μM iron (added as $FeCl_3$–Na nitrilotriacetate, Fe–NTA) displayed hypertrophy features that included increased protein synthesis and cell size, plus realignment of F-actin filaments along with sarcomeres and activation of the atrial natriuretic factor gene promoter. Incubation with higher Fe–NTA concentrations (100 μM) produced cardiomyocyte death by necrosis. Incubation for 24 h with Fe–NTA (20–40 μM) or the nitric oxide donor Δ-nonoate increased iNOS mRNA but decreased iNOS protein levels; under these conditions, iron stimulated the activity and the dimerization of iNOS. Fe–NTA (20 μM) promoted short- and long-term generation of reactive oxygen species, whereas preincubation with L-arginine suppressed this response. Preincubation with 20 μM Fe–NTA also attenuated the necrotic cell death triggered by 100 μM Fe–NTA, suggesting that these preincubation conditions have cardioprotective effects. Inhibition of iNOS activity with 1400 W enhanced iron-induced ROS generation and prevented both iron-dependent cardiomyocyte hypertrophy and cardioprotection. In conclusion, we propose that Fe–NTA (20 μM) stimulates iNOS activity and that the enhanced NO production, by promoting hypertrophy and enhancing survival mechanisms through ROS reduction, is beneficial to cardiomyocytes. At higher concentrations, however, iron triggers cardiomyocyte death by necrosis.

In animal models, cardiac muscle iron overload promotes systolic and diastolic abnormalities, cardiac fibrosis, and cardiac hypertrophy, leading to myocardial dysfunction [1,2]. Through the Haber Weiss and Fenton reactions iron mediates the production of superoxide ($O_2^{\bullet -}$) and hydroxyl ($^{\cdot}OH$) radicals [3]; overproduction of these reactive oxygen species (ROS) causes cell death [4]. In addition, $O_2^{\bullet -}$ can react with nitric oxide (NO) to generate peroxynitrite, which can either kill cells [5] or exert a protective role in cardiac or cerebral ischemic preconditioning [6].

NO is generated from L-arginine by three nitric oxide synthase (NOS) isoforms [7]. All three NOS isoforms are present in cardiac muscle and play key roles in cardiac function [8]. Activation of eNOS and iNOS expression is important for exercise-induced cardiac preconditioning, an effect prevented by antioxidants [9]. Moreover, eNOS knockout mice display increased infarct size after ischemia/reperfusion [10], supporting a protective role for eNOS in cardiac function. In contrast, iNOS overexpression generates peroxynitrite and causes sudden death [11], whereas iNOS-deficient transgenic mice show increased survival after ischemia and reperfusion [12]. Furthermore, specific iNOS overexpression induces cardiac hypertrophy and fibrosis [13].

Cellular ROS are involved in the transcriptional activation of iNOS and play a key role in cardiac protection [13]. Up to a certain level, ROS generation has a pivotal role in cell survival, preconditioning, and cardiac hypertrophy [14]. Because cardiomyocytes are terminally differentiated cells that have lost the ability to proliferate, cardiac growth during hypertrophy results primarily from an increase in cellular protein content, with little or no change in cardiomyocyte number [15]. The development of hypertrophy involves cytoskeletal reorganization, metabolic adaptation, increased protein synthesis (i.e., β-myosin heavy chain, β-MHC), activation of a fetal program of gene expression (i.e., atrial natriuretic factor, ANF), and expression of antiapoptotic proteins [15]. Hypertrophy can be initially considered,

* Corresponding authors. J.P. Munoz is to be contacted at Centro FONDAP de Estudios Moleculares de la Célula. S. Lavandero, Departamento de Bioquímica y Biología Molecular, Facultad Ciencias Químicas y Farmacéuticas. Fax: +562 678 2912.
E-mail addresses: jpablo_munoz@yahoo.com (J.P. Munoz), slavander@uchile.cl (S. Lavandero).

therefore, an adaptive mechanism that protects cardiomyocytes against cell death.

We studied the effects of iron on the induction of cardiomyocyte survival and death and investigated how NO, iNOS, and ROS participate in these effects. We show here for the first time that incubation of cultured cardiomyocytes with 20 μM $FeCl_3$–sodium nitrilotriacetate (Fe–NTA) stimulates hypertrophy and promotes survival, whereas higher iron concentrations (80–100 μM) produce necrosis. Fe–NTA (20–60 μM) stimulated the generation of NO and nitrate/nitrite metabolites. Inhibition of iNOS activity increased iron-induced ROS generation and prevented cardiomyocyte hypertrophy as well as iron-dependent cardioprotection. We propose that 20 μM Fe–NTA stimulates iNOS activity and that the ensuing NO production is beneficial in promoting hypertrophy and enhancing survival mechanisms in cardiomyocytes.

Experimental methods

Culture of cardiomyocytes and iron challenge

All studies conformed to the *Guide for the Care and Use of Laboratory Animals*, published by the U.S. National Institutes of Health (NIH, Publication No. 85-23, revised in 1996), and were approved by the Institutional Ethics Review Committee, Facultad de Ciencias Químicas y Farmacéuticas, Universidad de Chile. Cardiomyocytes were isolated from neonatal Sprague–Dawley rat ventricles as described previously [16]. Rats were bred in the Animal Breeding Facility of the Facultad de Ciencias Químicas y Farmacéuticas, Universidad de Chile. Cell cultures were at least 95% pure. Cardiomyocytes were plated at 70% final density on gelatin-coated petri dishes and maintained for 24 h in DMEM/M199 (4/1), 10% fetal bovine serum (FBS), 5% fetal calf serum (FCS). Serum was withdrawn 24 h before the cells were further incubated with 20–100 μM Fe^{3+} as the complex Fe–NTA (1:2.2, mol:mol) [17], 100 μM desferoxamine, or 200 μM Δ-nonoate at 37°C. For iNOS inhibition, cardiomyocytes were preincubated with 10 μM 1400 W before incubation with iron.

Cytotoxicity assays

Cardiomyocyte viability was evaluated using the trypan blue exclusion method [18]. Necrosis was quantified by measuring lactate dehydrogenase (LDH) activity in cells and culture media using the Sigma LDH kit. The fraction of LDH released was determined by comparing LDH activity in culture medium relative to total LDH activity.

Apoptosis assays

Mitochondrial transmembrane potential was measured after loading cardiomyocytes with tetramethylrhodamine methyl ester (TMRM; 100 nM, used in nonquench mode) and cell fluorescence was determined by flow cytometry ($\lambda_{excitation} = 543$ nm; $\lambda_{emission} = 560$ nm) using a FACScan system (Becton–Dickinson, San Jose, CA, USA). DNA fragmentation was determined in cardiomyocytes permeabilized with methanol and labeled with propidium iodide (PI) and the sub-G1 population was quantified by flow cytometry.

Cardiomyocytes grown on coverslips were fixed with PBS containing 4% paraformaldehyde for 10 min, permeabilized with 0.3% Triton X-100 for 10 min, and blocked for 1 h with 5% BSA in PBS. Cells were then incubated with anti-cytochrome *c* antibody (BD Pharmingen) at 1:400 and revealed with anti-mouse IgG–Alexa 488. Coverslips were mounted in DakoCytomation fluorescence mounting medium (DakoCytomation) and visualized by confocal microscope (Carl Zeiss Axiovert 135, LSM Microsystems). Procaspase 3 fragmentation was determined by Western blot using anti-caspase 3 antibody (Cell Signaling) and secondary HRP-coupled antibody (Calbiochem) and developed by chemiluminescence using the ECL system (Perkin–Elmer). As a positive control cells were incubated with 300 mM sorbitol for 6 h [18].

Assays of cardiomyocyte hypertrophy

Sarcomerization was determined by confocal microscopy analysis (Carl Zeiss Axiovert 135, LSM Microsystems) of methanol-permeabilized cells stained with TOPRO3 1:400 (to stain nuclei) and phalloidin–rhodamine 1:400 (to stain F-actin). Quantitative analysis of sarcomeres was performed rating cardiomyocytes as having parallel bundles or complete disorganization, diffuse or punctate staining. Cardiomyocyte size was determined in methanol-permeabilized cells stained with β-MHC antibody (1:80) and anti-rabbit–FITC. At least 100 cells from randomly selected fields were analyzed using the ImageJ software (NIH). ANF promoter expression was assessed using the ANF-lux reporter plasmid provided by Dr. K.R. Chien (Harvard Medical School, Boston, MA, USA) and was normalized against the pRL-TK reporter plasmid (Promega, Madison, WI, USA). Protein synthesis was evaluated through the incorporation of [^{3}H]phenylalanine (1 μCi/μl) on trichloroacetic acid-insoluble protein.

Evaluation of iNOS activity and mRNA and protein levels

iNOS activity was determined according to Balligand et al. [19]. Briefly, cardiac myocytes, plated on 60-mm dishes at 60% confluence, were washed with PBS and homogenized with 200 μl of a solution containing 20 mM Tris–HCl, pH 7.4, 0.5 mM EDTA, 1 mM dithiothreitol (DTT), 1 μM tetrahydrobiopterin, 1 μM leupeptin, 0.2 mM phenylmethylsulfonyl fluoride. Homogenates were incubated for 15 min on ice, sonicated for 30 s, and centrifuged at 1500 *g* for 15 min at 4°C. Protein concentrations were determined by the Bradford method. One hundred micrograms of protein (in 25 μl) was added to 125 μl of assay solution (50 mM Tris–HCl, pH 7.4, 1 mM EDTA, 1 mM EGTA, 0.5 mM NADPH, 10 μM FAD, 10 μM FMN, 10 μM tetrahydrobiopterin, 1 mM DTT, 100 mM NaCl, 10 μg/ml calmodulin, and 0.2 mM L-[^{3}H]arginine (61 Ci/mmol; Amersham)) and incubated for 1 h at 37°C. Samples were applied to Dowex 50 W8-400 ion-exchange resin preequilibrated with 20 mM Hepes, pH 5.5. The product L-[^{3}H]citrulline was eluted with deionized water. Radioactivity was quantified by scintillation counting.

RNA was isolated from cardiomyocytes using Trizol reagent. cDNA was obtained with reverse transcriptase and random primers. iNOS forward and reverse primers were 5′-GGGATCTTGGAGCGAGTTGTGG-3′ and 5′-TCTGCCTGTGCGTCTCTTCCG-3′, respectively. For β-actin, the primers were 5′-TCTACAATGAGCTGCGTGTG-3′ and 5′-TACATGGCTGGGGTGTTGAA-3′, respectively. Thermal cycling conditions were 94°C for 3 min, followed by 30 cycles at 94°C for 45 s, 56°C for 30 s, and 72°C for 30 s, and the final extension reaction was done at 72°C for 7 min. Total protein extracts from cardiomyocytes were resolved by SDS–PAGE; gels were electrotransferred to nitrocellulose and blocked with 5% nonfat milk in PBS plus 0.05% (v/v) Tween 20. Blots were incubated with iNOS antibody (1:1000) and then horseradish peroxidase-linked secondary antibody (1:5000) and revealed by enhanced chemiluminescence reagent. Blots were quantified by densitometry, using tubulin as loading control. iNOS dimer levels were analyzed by Western blot under nonreducing conditions as described previously [20].

Measurement of ROS

Plated cardiomyocytes were incubated for 24 h with 0–40 μM Fe–NTA, preloaded with DCDHF-DA in Krebs buffer, incubated for 10 min, and washed with PBS. ROS generation was measured at 37°C in a fluorimetric plate reader ($\lambda_{excitation} = 485$ nm; $\lambda_{emission} = 535$ nm) for 90 min. ROS generation was also determined in trypsin-treated

cardiomyocytes loaded with 25 μM dihydrorhodamine 123 for 30 min and then subjected to flow cytometry ($\lambda_{excitation} = 543$ nm; $\lambda_{emission} = 560$ nm) in a FACS Scan (Becton–Dickinson).

Expression of results and statistical methods

Data are presented either as means ± SEM of a number (n) of independent experiments or as examples of representative experiments performed on at least three separate occasions. Data were analyzed by analysis of variance and comparisons between groups were performed using a protected Tukey t test. A value of $p<0.05$ was chosen as the limit of statistical significance.

Results

High iron concentrations stimulate necrosis in cultured cardiomyocytes

Incubation with 20 to 60 μM Fe–NTA for 24 h did not affect cardiomyocyte viability, whereas 80 or 100 μM Fe–NTA resulted in around 2.5-fold increase in cell death (Fig. 1A). Twenty to 60 μM Fe–NTA did not modify significantly LDH release relative to the controls. In contrast, 80 or 100 μM Fe–NTA increased LDH release 1.4- and 2-fold over control (Fig. 1B), suggesting significant cell necrosis under these conditions. Mitochondrial transmembrane potential determined by TMRM fluorescence decreased by 20–30% after 8 h of incubation with

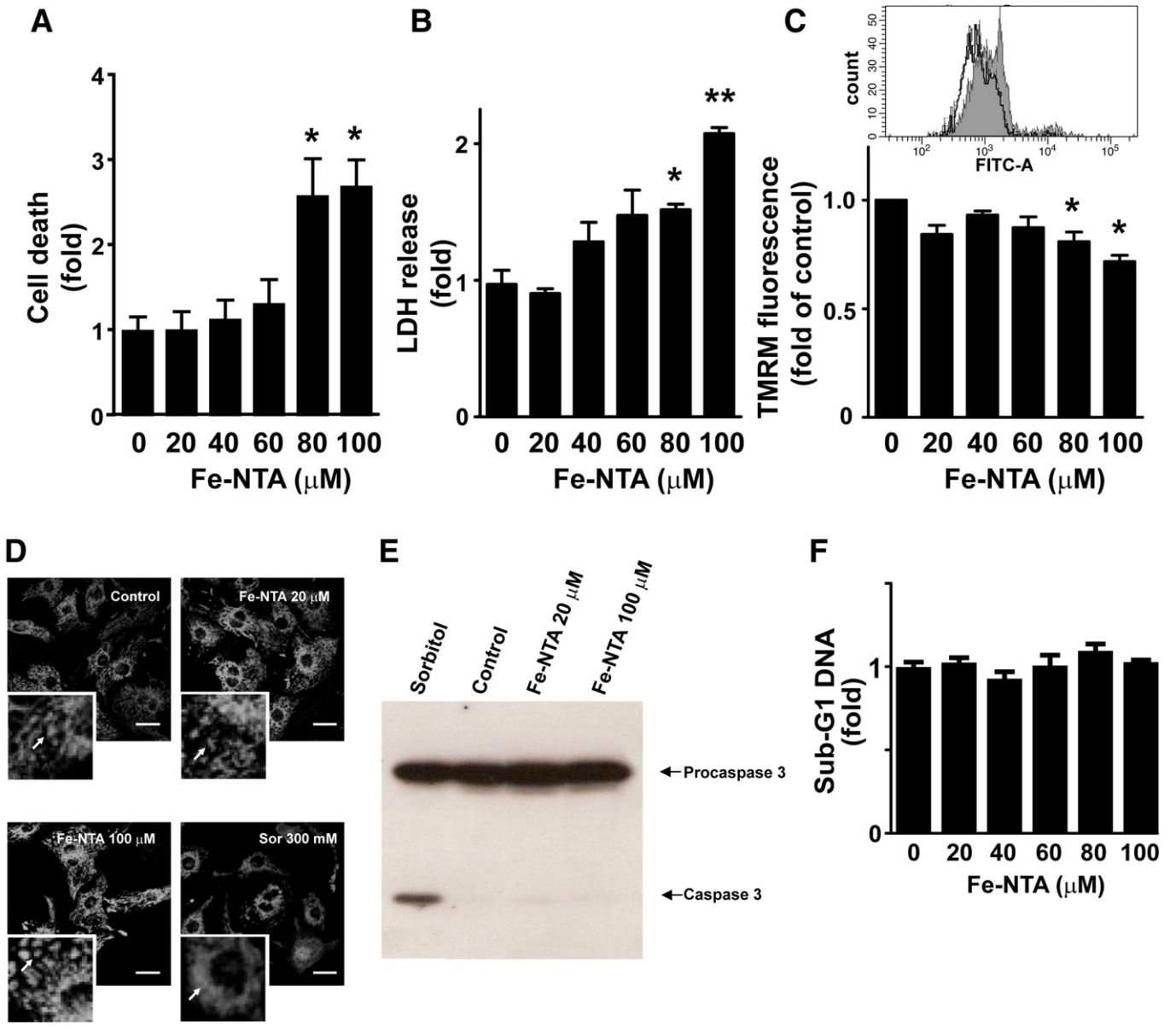

Fig. 1. High iron concentrations induce cell death in cultured cardiomyocytes. (A) Cells were incubated with 0–100 μM Fe–NTA for 24 h and cell death was assessed using the trypan blue exclusion method. Data are given as means ± SEM ($n = 8$). *$p<0.05$ vs 0 μM Fe–NTA. (B) Cells were incubated with 0–100 μM Fe–NTA for 24 h and necrosis was determined by the extent of LDH release into the culture medium. Data represent means ± SEM ($n = 3$). *$p<0.05$ and **$p<0.01$ vs 0 μM Fe–NTA. (C) Cells were incubated with 0–100 μM Fe–NTA for 8 h and mitochondrial potential was assessed by flow cytometry using TMRM as the fluorescent probe. The top shows representative TMRM fluorescence plots obtained from control cells (gray line) or from cells incubated with 100 μM Fe–NTA (black line), and the bottom shows the values obtained at 0–100 μM Fe–NTA, given as means ± SEM ($n = 3$). *$p<0.05$ vs 0 μM Fe–NTA. (D) Cells were incubated with 0, 20, or 100 μM Fe–NTA for 8 h and cytochrome c was detected by immunocytochemistry using anti-cytochrome c with FITC-conjugated secondary antibody (green). Sorbitol (300 mM) was used as positive control. Insets are close-ups of images. Arrows show punctate or diffuse cytochrome c labeling. (E) Cells were incubated with 0, 20, or 100 μM Fe–NTA for 2 h and procaspase and caspase 3 were detected by Western blot. Sorbitol (300 mM) was used as positive control. (F) Cells were incubated with 0–100 μM Fe–NTA for 24 h and DNA fragmentation was detected by measuring sub-G1 DNA with PI labeling followed by flow cytometry in permeabilized cells. Data represent means ± SEM ($n = 3$).

80–100 μM Fe–NTA, but was not affected significantly by lower iron concentrations (Fig. 1C). Cardiomyocytes incubated with 20–100 μM Fe–NTA did not undergo apoptosis as evaluated by mitochondrial cytochrome *c* release (Fig. 1D), caspase 3 activation (Fig. 1E), and DNA fragmentation (Fig. 1F). Hyperosmotic stress produced by sorbitol (300 mM) was used as positive control for mitochondrial cytochrome *c* release and caspase 3 activation (Figs. 1D and 1E). These results suggest that 20 μM Fe–NTA does not induce cell death, whereas 80–100 μM Fe–NTA stimulates cardiomyocyte death by promoting necrosis but not apoptosis.

Fe–NTA (20 μM) induces cardiomyocyte hypertrophy

Cardiomyocytes (β-MHC-positive cells) incubated for 24 h with 20 μM Fe–NTA presented a 30% increase in cell area (Fig. 2A), plus greater than twofold enhanced ANF-reporter gene activity (Fig. 2B), without changes in DNA content (Supplementary Fig. 1), and displayed a 20% increase in [^{3}H]phenylalanine incorporation (Fig. 2C). Moreover, cardiomyocytes incubated for 24 h with 20 μM Fe–NTA presented 60% sarcomerized F-actin, compared to the controls, which had only 16% sarcomerized F-actin (Fig. 2D). These

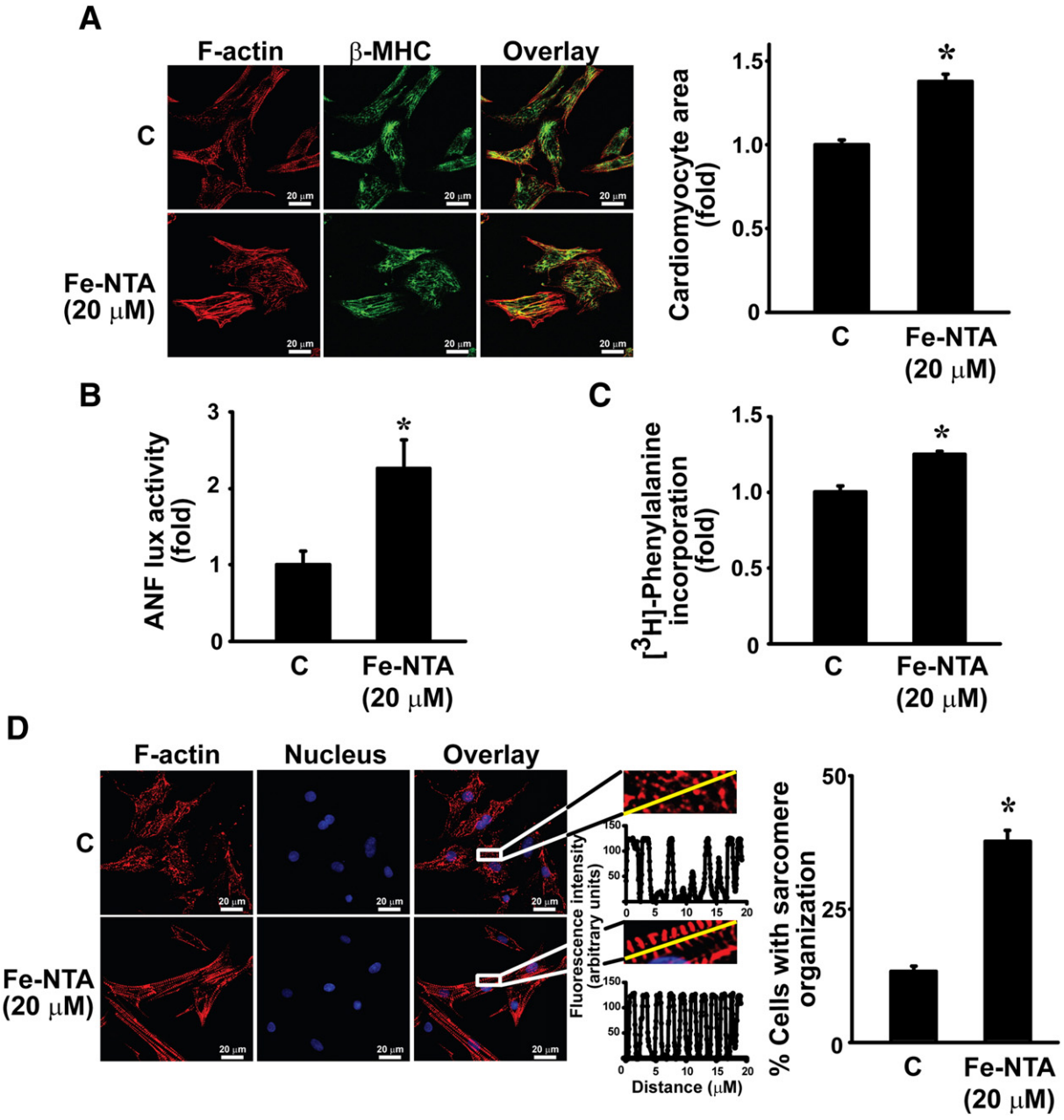

Fig. 2. Low iron concentration induces hypertrophy in cultured cardiomyocytes. Cells were incubated with or without 20 μM Fe–NTA for 24 h. (A) Left: F-actin filaments were stained with rhodamine-conjugated phalloidin (red) and β-MHC was detected using anti-β-MHC with FITC-conjugated secondary antibody (green). Right: cardiomyocyte area was determined in 100 cells for each condition. Data are given as means ± SEM ($n = 4$); *$p < 0.05$ vs control (C). (B) ANF-promoter activity in iron-incubated cardiomyocytes. Cells were transfected with ANF-lux and TK-*Renilla* reporter gene plasmids, and luciferase activity was determined by luminescence. Results were expressed as lux/*Renilla* ratio. Data represent means ± SEM ($n = 5$); *$p < 0.05$ vs control. (C) Protein synthesis was assessed by [^{3}H]phenylalanine incorporation in cardiomyocytes incubated with or without 20 μM Fe–NTA. Data represent means ± SEM ($n = 3$); *$p < 0.05$ vs control. (D) Cell sarcomerization was visualized by F-actin filament labeling with rhodamine-conjugated phalloidin (red). Nuclei were stained with Hoechst (blue). Insets show sarcomerization details (left). The percentage of sarcomerized cardiomyocytes was determined by counting 100 cells from three independent experiments (right). Data represent means ± SEM; *$p < 0.05$ vs control.

results suggest that 20 μM Fe–NTA effectively induces hypertrophy in cultured cardiomyocytes. At higher Fe–NTA concentrations, i.e., 80 μM, some of the surviving cardiac myocytes displayed increased cell size and sarcomerization (data not shown), suggesting that hypertrophy and cell death occur simultaneously under these conditions.

Iron stimulates NO generation in cardiomyocytes

Cardiomyocytes were incubated with nonlethal iron concentrations (20–40 μM Fe–NTA), and NOS activity was indirectly measured through the formation of L-[^{3}H]citrulline. Incubation of cardiomyocytes with 20 μM Fe–NTA for 24 h increased L-[^{3}H]citrulline formation approximately threefold (Fig. 3A). NO generation was also measured using the fluorescent specific NO probe DAF-FM [21]. A time series of confocal microscopy images of live cardiomyocytes preloaded with DAF-FM showed that, up to 60 min, NO generation increased significantly after 40 or 60 μM Fe–NTA addition (Supplementary Figs. 2A and 2B) and was decreased by 40% with the specific iNOS inhibitor 1400W (data not shown). These results suggest that iNOS plus other NOS isoforms contributes to iron-dependent NO generation.

NO regulates iNOS protein levels in cultured cardiomyocytes

A significant decrease in iNOS protein content was observed after 12 h of incubation of cardiomyocytes with 20 μM Fe–NTA (Fig. 3B);

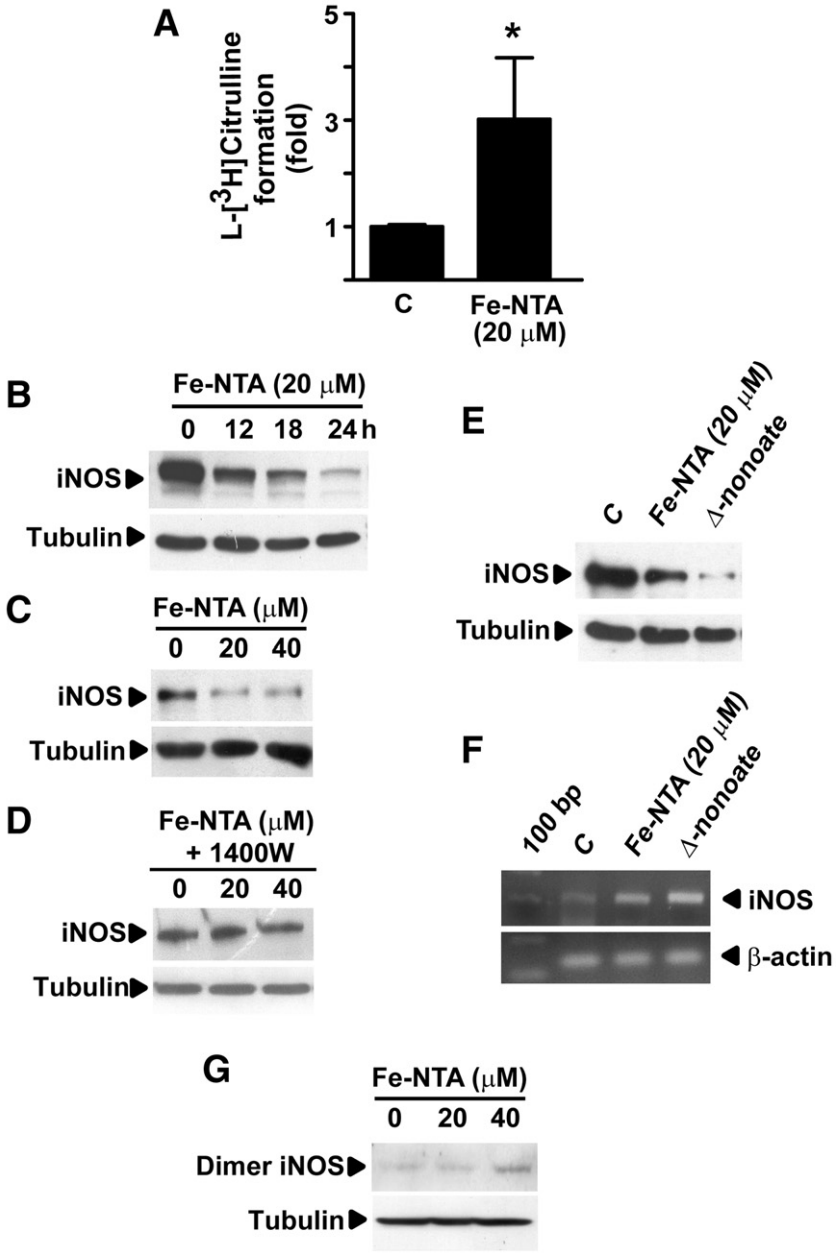

Fig. 3. iNOS contributes to nitric oxide generation and nitric oxide induces iNOS degradation in cultured cardiomyocytes incubated with iron. (A) iNOS activity, measured as L-[^{3}H] citrulline formation, in cardiac myocytes incubated with 20 μM Fe–NTA for 24 h. Data are given as means ± SEM ($n = 3$); *$p < 0.05$ vs control. (B) Time course of iNOS monomer protein changes in cells after incubation with 20 μM Fe–NTA for 0–24 h. (C) iNOS monomer protein content after incubation with 0–40 μM Fe–NTA for 24 h. (D) Effect of 10 μM 1400W on iNOS monomer protein content after incubation with 0–40 μM Fe–NTA for 24 h. Representative Western blots for iNOS with tubulin as loading control are shown ($n = 3$). (E and F) Representative blots of iNOS monomer protein ($n = 3$) and iNOS mRNA levels ($n = 3$), respectively, obtained for cardiomyocytes incubated with 20 μM Fe–NTA or 200 μM Δ-nonoate for 24 h. (G) iNOS dimer protein content in cardiomyocytes incubated with 0–40 mM Fe–NTA for 24 h ($n = 3$) was determined as described under Experimental methods.

this decrease was more pronounced after 18 h of incubation, whereas after 24 h iNOS decreased to very low levels (Fig. 3B). The substantial decrease in iNOS protein levels produced by 24 h incubation with 20 μM Fe–NTA was similar to that observed after incubation with 40 μM Fe–NTA (Fig. 3C). Despite the significant decrease in iNOS protein levels, total NOS activity measured as L-[^{3}H]citrulline production was around threefold higher in cells preincubated for 24 h with 20 μM Fe–NTA than in controls (Fig. 3A).

To investigate whether iNOS-generated NO promoted cytoplasmic iNOS degradation, cardiomyocytes were incubated with 20–40 μM Fe–NTA for 24 h in the presence of 1400W. Fig. 3D shows that 1400W largely prevented the iNOS protein decrease produced by 24 h incubation with 20–40 μM Fe–NTA. To further study whether NO generation promoted iNOS degradation, cells were incubated for 24 h with the NO donor Δ-nonoate to increase NO levels. Fig. 3E shows that Δ-nonoate drastically decreased iNOS protein levels, suggesting that

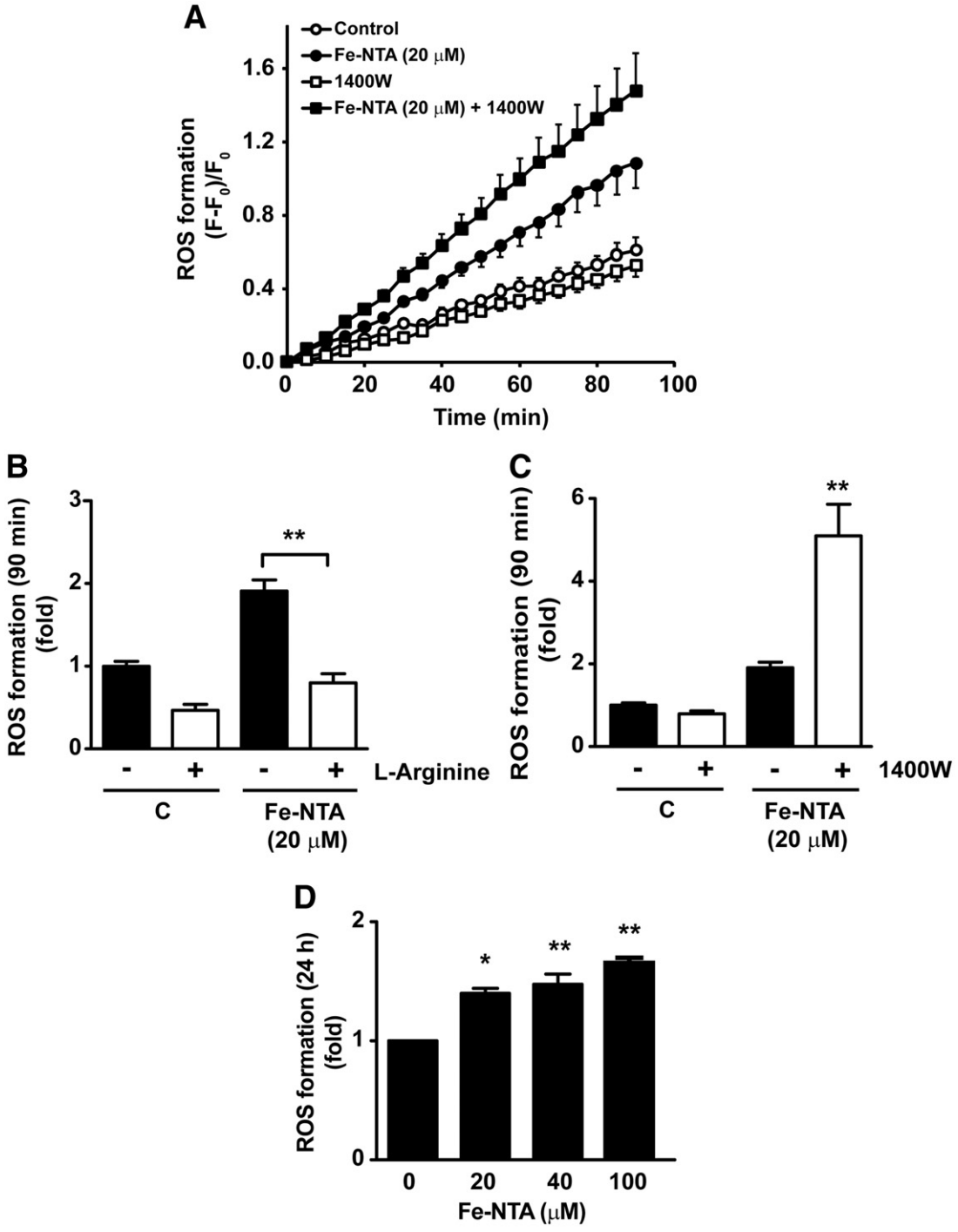

Fig. 4. Iron-induced nitric oxide decreases ROS formation in cultured cardiomyocytes. (A) Cells were loaded with DCDHF-DA (10 μM) and incubated with 20 μM Fe–NTA for 90 min in Krebs buffer in the presence or absence of 10 μM 1400W. ROS formation was monitored continuously using a plate reader spectrofluorimeter. Data represent means ± SEM ($n = 6$). (B) ROS generation in cells incubated with 20 μM Fe–NTA for 90 min, in the presence and absence of 100 μM L-arginine. Data represent means ± SEM ($n = 6$); $^{**}p < 0.01$ vs 20 μM Fe–NTA. (C) ROS generation in cells incubated with 20 μM Fe–NTA for 90 min, in the presence or absence of 10 μM 1400W. Data represent means ± SEM ($n = 8$); $^{**}p < 0.01$ vs 20 μM Fe–NTA and C. (D) Cells were supplemented with 0, 20, 40, or 100 μM Fe–NTA, incubated for 24 h, and loaded with dihydrorhodamine 123 for 30 min. ROS formation was detected by flow cytometry. Data are given as means ± SEM ($n = 6$); $^{*}p < 0.05$, $^{**}p < 0.01$ vs 0 μM Fe–NTA.

enhanced NO generation causes almost complete iNOS depletion. Yet, cardiomyocytes incubated for 24 h with 20 μM Fe–NTA or Δ-nonoate displayed increased iNOS mRNA levels relative to the control (Fig. 3F). Thus, a decrease in transcript level seems not to be the cause of the marked decrease in iNOS protein content produced by 24 h incubation with 20 μM Fe–NTA or Δ-nonoate.

These results combined show that 20–40 μM Fe–NTA increased NO generation at early times but at later times decreased iNOS protein content by promoting cytoplasmic iNOS depletion. Thus, iNOS-generated NO may contribute to the down-regulation of iNOS protein levels in iron-stressed cardiomyocytes.

To explore why Fe–NTA produced an increase in iNOS activity despite the significant iNOS protein reduction, we investigated whether Fe–NTA increased iNOS dimerization as reported by Chen et al. [22]. Fig. 3G shows that 20–40 μM Fe–NTA increased iNOS dimer levels. These data suggest that enhanced iNOS dimerization is responsible for the increase in iNOS enzymatic activity induced by Fe–NTA.

NO release decreases ROS generation in iron-incubated cells

Significant endogenous ROS generation, which increased linearly up to 90 min, was observed in control cardiomyocytes preloaded with DCDHF-DA; addition of 20 μM Fe–NTA increased by 1.8-fold the rate of ROS production (Fig. 4A). L-Arginine decreased ROS generation to control levels in cells incubated with 20 μM Fe–NTA for 90 min (Fig. 4B). Moreover, cells incubated with 20 μM Fe–NTA and 1400W exhibited a significant increase in ROS production compared to control cells (Figs. 4A and 4C). These results suggest that NO produced via iron-induced iNOS activation reduced ROS formation in cardiomyocytes.

In analogy to the results obtained after incubation with iron for 90 min, incubation with 20 μM Fe–NTA for 24 h significantly increased ROS formation; but increasing iron concentration to 40 or 100 μM Fe–NTA did not enhance ROS generation further (Fig. 4D).

The results illustrated in Figs. 3 and 4 indicate that short (90 min) and long (24 h) incubations with 20 μM Fe–NTA stimulate production of both ROS and NO in cultured cardiomyocytes.

Low iron concentration induces cardiomyocyte survival and hypertrophy through an iNOS-dependent mechanism

To investigate whether low iron concentration (20 μM Fe–NTA) provided protection against the loss of viability produced by higher Fe–NTA concentrations, cells were preincubated for 24 h with or without 20 μM Fe–NTA, followed by 24 h exposure to 100 μM Fe–NTA. Treatment with 100 μM Fe–NTA induced around threefold increase in cell death, but preincubation with 20 μM Fe–NTA drastically reduced the cardiomyocyte death induced by 100 μM Fe–NTA (Fig. 5A, top). A similar result was obtained when LDH release (a necrotic cell death marker) was determined (Fig. 5A, bottom). Moreover, preincubation with 10 μM 1400W completely abolished the protective action of 20 μM Fe–NTA pretreatment (Figs. 5A and 5B), suggesting an iNOS-dependent mechanism. These results suggest that preincubation with 20 μM Fe–NTA significantly attenuated the cardiomyocyte necrotic death induced by 100 μM Fe–NTA by an iNOS-dependent mechanism.

As shown in Fig. 2, cell incubation for 24 h with 20 μM Fe–NTA induced a hypertrophic response. To assess the contribution of iNOS to hypertrophy, cardiomyocytes were preincubated for 24 h with 20 μM Fe–NTA in the presence or absence of 10 μM 1400W. Inhibition of iNOS with 1400W prevented the increase in cellular area produced by 20 μM Fe–NTA (Fig. 5B, top). Incubation of cardiomyocytes with 20 μM Fe–NTA for 24 h also stimulated the ANF-lux reporter gene, a hypertrophy marker that measures the activation of the prohypertrophic gene expression program; iNOS

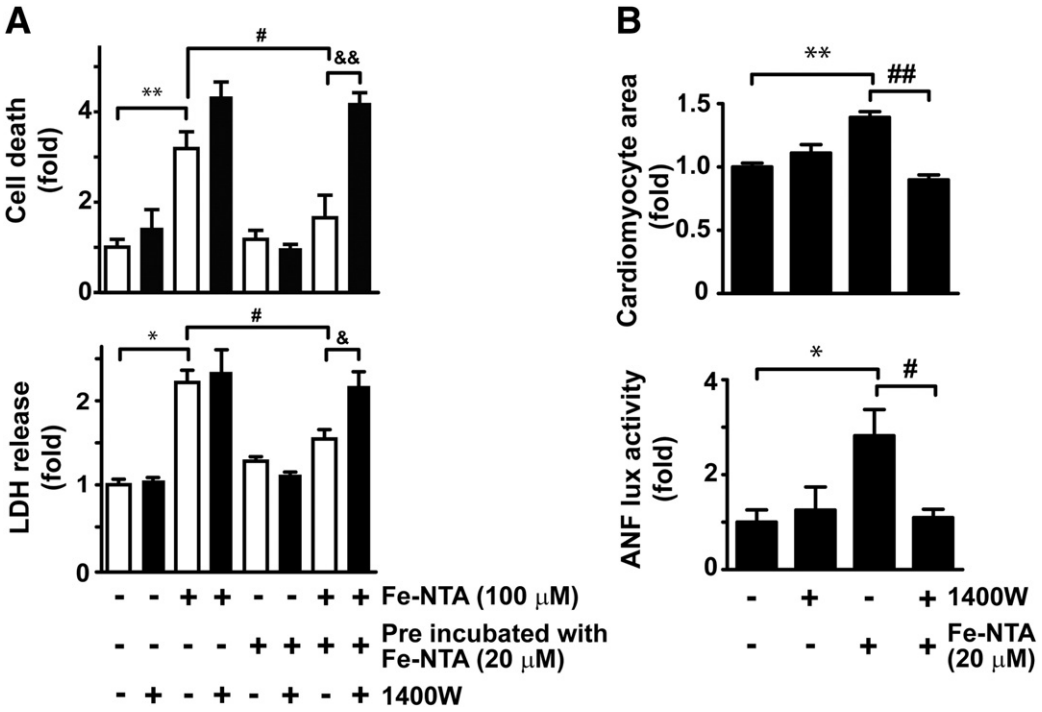

Fig. 5. Low iron concentration induces cardiomyocyte survival and hypertrophy through an iNOS-dependent mechanism. (A) Cells were preincubated with 20 μM Fe–NTA for 24 h, incubated with or without 10 μM 1400W for 60 min, and then incubated with 100 μM Fe–NTA for 24 h. Top: Cell viability was assessed with the trypan blue exclusion method. Data represent means ± SEM ($n = 6$); $^{**}p < 0.01$ vs control, $^{\#}p < 0.05$ vs 100 μM Fe–NTA, and $^{\&\&}p < 0.01$ vs preincubation with 20 μM Fe–NTA plus 100 μM Fe–NTA. Bottom: Necrosis was determined by LDH release into the culture medium. Data represent means ± SEM ($n = 3$); $^{*}p < 0.05$ vs control, $^{\#}p < 0.05$ vs 100 μM Fe–NTA, and $^{\&}p < 0.05$ vs preincubation with 20 μM Fe–NTA plus 100 μM Fe–NTA. (B) Cells were incubated with or without 10 μM 1400W for 60 min and then with 20 μM Fe–NTA for 24 h. Cardiomyocyte area was determined in 100 cells for each condition (top). Cells were transfected with the ANF-lux reporter gene and incubated with or without 10 μM 1400 W for 60 min and then with 20 μM Fe–NTA for 24 h; the ANF-lux reporter activity is shown at the bottom. Data are means ± SEM ($n = 4$); $^{*}p < 0.05$ and $^{**}p < 0.01$ vs control, $^{\#}p < 0.05$ and $^{\#\#}p < 0.01$ vs 20 μM Fe–NTA.

inhibition by 1400W prevented the stimulating effect of 20 μM Fe–NTA (Fig. 5A, bottom). These results suggest that 20 μM Fe–NTA induces cardiomyocyte hypertrophy by promoting NO generation via iNOS.

Discussion

The main findings presented in this work are: (a) high Fe–NTA concentrations (80–100 μM) induced cardiomyocyte death by necrosis and lower Fe–NTA concentrations (20 μM) stimulated both cardiomyocyte hypertrophy and cardioprotection; (b) iron-induced NO generation was required for iron-dependent hypertrophy and cardioprotection; and (c) iron (20–40 μM) stimulated iNOS mRNA expression, iNOS enzymatic activity, and iNOS dimerization, but decreased iNOS protein content.

Iron cardiotoxicity has been described in animal models as well as in patients with primary hemochromatosis, β-thalassemia, and end-stage kidney disease [23–25]. Echocardiography evaluations performed in patients with idiopathic hemochromatosis showed that increased thickness of ventricular walls without impairment of left ventricular systolic function is probably the first and still reversible cardiac alteration due to iron deposition in the myocardium [26]. Later, with increasing iron overload, left ventricular function becomes impaired and dilated cardiomyopathy develops [26]. During iron overload, lipid peroxidation increases the content of unsaturated and saturated aldehydes in the heart and plasma [25,27]. These agents are associated with cell dysfunction, cytotoxicity, and death [23]. In a rat model of heart ischemia and reperfusion, intraperitoneal administration of iron reduces the postischemic recovery of heart function, associated with increased hydroperoxide content in heart perfusates [28]. These observations agree with our data showing that low Fe–NTA (20–40 μM) concentrations triggered cardiomyocyte hypertrophy, i.e., similar to the initial stages of hemochromatosis, whereas high concentrations of Fe–NTA (80–100 μM) triggered cardiomyocyte death, similar to the effects of iron overload.

In rats, iron depletion caused by a single administration of the specific iron chelator desferoxamine (200 mg/kg) induces prolonged myocardial preconditioning via accumulation of oxygen radicals through a NOS-dependent mechanism [29]. Similar results were also obtained in isolated rabbit hearts and cultured rabbit cardiomyocytes [30]. Here, we show that low iron concentrations triggered both cardiac hypertrophy and cardioprotection. Stimuli that trigger hypertrophy can induce the expression of antiapoptotic proteins such as Bcl-2 and survivin, and a recent report has shown that the hypertrophic agents ET-1 and LIF decrease H_2O_2-induced necrosis [31,32]. Our results, showing that iron at low concentrations protected against necrosis induced by higher iron concentrations, agree with a report showing that in vascular smooth muscle cells HSP72 and HSP27 participate in protection against necrosis but not against apoptosis [33].

We show here that iron stimulated NO synthesis in cultured cardiomyocytes. A number of studies have described a complex interrelationship between iron and NO, which can result in changes in NO production in vivo [34]. In this regard, increased NO generation occurs in the liver under conditions of acute and chronic iron overload [35]. In patients with hereditary hemochromatosis a higher expression of liver iNOS was observed, whereas iron enhances NO production in cultured proximal tubule cells [36].

Using the potent inhibitor of iNOS 1400 W, we show here that iNOS contributes to iron-dependent NO synthesis. The inhibitory activity of 1400W against iNOS is about 5000- and 200-fold more effective than against eNOS and nNOS, respectively [37]. Several agents, including statins and phosphodiesterase-5 inhibitors, can induce iNOS activity in the heart, in which their most significant action is linked to late preconditioning [8,38]. In this phase, eNOS-derived NO initiates a cascade of molecular events that culminates in the delayed activation of iNOS, which then confers protection [39]. Our results—showing that iNOS inhibition by 1400W abolished both the hypertrophic and the cardioprotective effects of low iron levels—suggest that iNOS-generated NO mediates iron-dependent hypertrophy and cardioprotection.

In an attempt to clarify the mechanism of iNOS activation by iron, the effects of 20 μM Fe–NTA on iNOS mRNA and protein content and enzymatic activity were investigated. We found that although iron-induced NO synthesis was associated with an increase in both iNOS mRNA and iNOS enzymatic activity, surprisingly, iron decreased iNOS protein content. This decrease required NO, because inhibition of iNOS-dependent NO synthesis increased iNOS protein content, whereas increased NO generation with Δ-nonoate had the opposite effect. The fact that iron increased iNOS mRNA levels suggests that the decreased iNOS protein content reflects increased iNOS protein degradation more than a reduction in its synthesis.

Different regulatory mechanisms have been proposed to control iNOS activity [40]; among them, it has been established that iNOS is activated by dimerization [22]. Heme, tetrahydrobiopterin (THB_4), L-arginine, and iNOS's own N-terminal region are all important stabilizers of iNOS dimeric structure [22,41]. NO produced from the reaction catalyzed by iNOS not only can rebind to the heme group, thereby directly inhibiting the turnover of the enzyme, but also can induce monomerization of functional dimers [41]. It has been shown that NO-induced monomers cannot revert to the dimeric state by the combined addition of L-arginine and THB_4 [22,40]. Therefore, iron-enhanced NO-dependent iNOS degradation may be caused by irreversible NO-induced iNOS monomerization. Interestingly, Tummala et al. [41] demonstrated by mass spectroscopy that eNOS is S-nitrosylated and that this posttranslational modification promotes eNOS stability. Our results, shown in Fig. 3G, support the hypothesis that Fe–NTA promotes iNOS dimerization in cardiomyocytes, possibly explaining the increase in iron-induced iNOS activity despite iNOS protein reduction.

Several reports have described that $O_2^{\bullet -}$ produced via NAPH oxidase, xanthine oxidase, and the mitochondria, plus H_2O_2 generated by monoamine oxidase, contributes to the development of cardiomyocyte hypertrophy [42]. A recent report showed that iNOS activity participates in hepatic regeneration and expression of survival proteins such as HSP70 and HO-1 [43]. Our findings indicate that low iron concentrations induce the activation of a cell protection program, which leads to hypertrophy via iNOS-dependent NO generation and the ensuing reduction of ROS levels. Additionally, cardiomyocyte iNOS down-regulates its own protein levels through NO formation, a cellular response that presumably counterbalances the strong activation of iNOS activity produced by iron.

In summary, our results indicate that the effects of iron on cardiomyocytes should be visualized as a biphasic response. Thus, depending on iron concentration cardiomyocytes can undergo cell death or can display instead cellular hypertrophy and activation of survival cascade pathways that require iNOS-mediated NO generation.

Acknowledgments

This work was supported by the Comisión Nacional de Ciencia y Tecnología (CONICYT, Chile) Program Fondo de Areas Prioritarias (FONDAP) (Grant 15010006 to S.L. and C.H.), Proyecto Postdoctorado (3060082 to J.P.M.), and Iniciativa Cientifica Milenio (P05001-F to M. T.N.). R.T., Z.P., B.T., J.D.E., and V.P. hold Ph.D. fellowships from CONICYT, Chile. We thank Fidel Albornoz and Ruth Marquez for their excellent technical assistance.

Appendix A. Supplementary data

Supplementary data associated with this article can be found, in the online version, at doi:10.1016/j.freeradbiomed.2009.11.017.

References

[1] Puntarulo, S. Iron, oxidative stress and human health. *Mol. Aspects Med.* **26:** 299–312; 2005.

[2] Yang, T.; Dong, W. Q.; Kuryshev, Y. A.; Obejero-Paz, C.; Levy, M. N.; Brittenham, G. M., et al. Bimodal cardiac dysfunction in an animal model of iron overload. *J. Lab. Clin. Med.* **140:**263–271; 2002.

[3] Halliwell, B. Biochemistry of oxidative stress. *Biochem. Soc. Trans.* **35:**1147–1150; 2007.

[4] Valko, M.; Morris, H.; Cronin, M. T. Metals, toxicity and oxidative stress. *Curr. Med. Chem* **12:**1161–1208; 2005.

[5] Thippeswamy, T.; McKay, J. S.; Quinn, J. P.; Morris, R. Nitric oxide, a biological double-faced Janus—is this good or bad? *Histol. Histopathol.* **21:**445–458; 2006.

[6] Kunz, A.; Park, L.; Abe, T.; Gallo, E. F.; Anrather, J.; Zhou, P., et al. Neurovascular protection by ischemic tolerance: role of nitric oxide and reactive oxygen species. *J. Neurosci.* **27:**7083–7093; 2007.

[7] Alderton, W. K.; Cooper, C. E.; Knowles, R. G. Nitric oxide synthases: structure, function and inhibition. *Biochem. J.* **357:**593–615; 2001.

[8] Massion, P. B.; Feron, O.; Dessy, C.; Balligand, J. L. Nitric oxide and cardiac function: ten years after, and continuing. *Circ. Res.* **93:**388–398; 2003.

[9] Akita, Y.; Otani, H.; Matsuhisa, S.; Kyoi, S.; Enoki, C.; Hattori, R., et al. Exercise-induced activation of cardiac sympathetic nerve triggers cardioprotection via redox-sensitive activation of eNOS and upregulation of iNOS. *Am. J. Physiol.* **292:** H2051–H2059; 2007.

[10] Sharp, B. R.; Jones, S. P.; Rimmer, D. M.; Lefer, D. J. Differential response to myocardial reperfusion injury in eNOS-deficient mice. *Am. J. Physiol.* **282:** H2422–H2426; 2002.

[11] Mungrue, I. N.; Gros, R.; You, X.; Pirani, A.; Azad, A.; Csont, T., et al. Cardiomyocyte overexpression of iNOS in mice results in peroxynitrite generation, heart block, and sudden death. *J. Clin. Invest.* **109:**735–743; 2002.

[12] Li, Q.; Guo, Y.; Tan, W.; Stein, A. B.; Dawn, B.; Wu, W. J., et al. Gene therapy with iNOS provides long-term protection against myocardial infarction without adverse functional consequences. *Am. J. Physiol.* **290:**H584–H589; 2006.

[13] Chen, C. H.; Chuang, J. H.; Liu, K.; Chan, J. Y. Nitric oxide triggers delayed anesthetic preconditioning-induced cardiac protection via activation of nuclear factor-kappaB and upregulation of inducible nitric oxide synthase. *Shock* **30:**241–249; 2008.

[14] Sawyer, D. B.; Siwik, D. A.; Xiao, L.; Pimentel, D. R.; Singh, K.; Colucci, W. S. Role of oxidative stress in myocardial hypertrophy and failure. *J. Mol. Cell. Cardiol.* **34:** 379–388; 2002.

[15] Heineke, J.; Molkentin, J. D. Regulation of cardiac hypertrophy by intracellular signalling pathways. *Nat. Rev. Mol. Cell. Biol.* **7:**589–600; 2006.

[16] Foncea, R.; Andersson, M.; Ketterman, A.; Blakesley, V.; Sapag-Hagar, M.; Sugden, P. H., et al. Insulin-like growth factor-I rapidly activates multiple signal transduction pathways in cultured rat cardiac myocytes. *J. Biol. Chem.* **272:**19115–19124; 1997.

[17] Aguirre, P.; Mena, N.; Tapia, V.; Arredondo, M.; Nunez, M. T. Iron homeostasis in neuronal cells: a role for IREG1. *BMC Neurosci.* **6:**3; 2005.

[18] Galvez, A. S.; Ulloa, J. A.; Chiong, M.; Criollo, A.; Eisner, V.; Barros, L. F., et al. Aldose reductase induced by hyperosmotic stress mediates cardiomyocyte apoptosis—differential effects of sorbitol and mannitol. *J. Biol. Chem.* **278:**38484–38494; 2003.

[19] Balligand, J. L.; Ungureanu-Longrois, D.; Simmons, W. W.; Pimental, D.; Malinski, T. A.; Kapturczak, M., et al. Cytokine-inducible nitric oxide synthase (iNOS) expression in cardiac myocytes: characterization and regulation of iNOS expression and detection of iNOS activity in single cardiac myocytes in vitro. *J. Biol. Chem.* **269:**27580–27588; 1994.

[20] Pieper, G. M.; Ionova, I. A.; Cooley, B. C.; Migrino, R. Q.; Khanna, A. K.; Whitsett, J., et al. Sepiapterin decreases acute rejection and apoptosis in cardiac transplants independently of changes in nitric oxide and inducible nitric-oxide synthase dimerization. *J. Pharmacol. Exp. Ther.* **329:**890–899; 2009.

[21] Lepiller, S.; Laurens, V.; Bouchot, A.; Herbomel, P.; Solary, E.; Chluba, J. Imaging of nitric oxide in a living vertebrate using a diamino-fluorescein probe. *Free Radic. Biol. Med.* **43:**619–627; 2007.

[22] Chen, Y.; Panda, K.; Stuehr, D. J. Control of nitric oxide synthase dimer assembly by a heme-NO-dependent mechanism. *Biochemistry* **41:**4618–4625; 2002.

[23] Eaton, J. W.; Qian, M. Molecular bases of cellular iron toxicity. *Free Radic. Biol. Med.* **32:**833–840; 2002.

[24] Livrea, M. A.; Tesoriere, L.; Pintaudi, A. M.; Calabrese, A.; Maggio, A.; Freisleben, H. J., et al. Oxidative stress and antioxidant status in beta-thalassemia major: iron overload and depletion of lipid-soluble antioxidants. *Blood* **88:**3608–3614; 1996.

[25] Young, I. S.; Trouton, T. G.; Torney, J. J.; McMaster, D.; Callender, M. E.; Trimble, E. R. Antioxidant status and lipid peroxidation in hereditary haemochromatosis. *Free Radic. Biol. Med.* **16:**393–397; 1994.

[26] Cecchetti, G.; Binda, A.; Piperno, A.; Nador, F.; Fargion, S.; Fiorelli, G. Cardiac alterations in 36 consecutive patients with idiopathic haemochromatosis: polygraphic and echocardiographic evaluation. *Eur. Heart J.* **12:**224–230; 1991.

[27] Esterbauer, H.; Schaur, R. J.; Zollner, H. Chemistry and biochemistry of 4-hydroxynonenal, malonaldehyde and related aldehydes. *Free Radic. Biol. Med.* **11:** 81–128; 1991.

[28] Kramer, J. H.; Lightfoot, F. G.; Weglicki, W. B. Cardiac tissue iron: effects on post-ischemic function and free radical production, and its possible role during preconditioning. *Cell. Mol. Biol.* **46:**1313–1327; 2000.

[29] Dendorfer, A.; Heidbreder, M.; Hellwig-Burgel, T.; Johren, O.; Qadri, F.; Dominiak, P. Deferoxamine induces prolonged cardiac preconditioning via accumulation of oxygen radicals. *Free Radic. Biol. Med.* **38:**117–124; 2005.

[30] Philipp, S.; Cui, L.; Ludolph, B.; Kelm, M.; Schulz, R.; Cohen, M. V., et al. Desferoxamine and ethyl-3,4-dihydroxybenzoate protect myocardium by activating NOS and generating mitochondrial ROS. *Am. J. Physiol. Heart Circ. Physiol.* **290:**H450–H457; 2006.

[31] Hahn, J. Y.; Cho, H. J.; Bae, J. W.; Yuk, H. S.; Kim, K. i.; Park, K. W., et al. beta-Catenin overexpression reduces myocardial infarct size through differential effects on cardiomyocytes and cardiac fibroblasts. *J. Biol. Chem.* **281:**30979–30989; 2006.

[32] Zhao, X. S.; Pan, W.; Bekeredjian, R.; Shohet, R. V. Endogenous endothelin-1 is required for cardiomyocyte survival in vivo. *Circulation* **114:**830–837; 2006.

[33] Champagne, M. J.; Dumas, P.; Orlov, S. N.; Bennett, M. R.; Hamet, P.; Tremblay, J. Protection against necrosis but not apoptosis by heat-stress proteins in vascular smooth muscle cells: evidence for distinct modes of cell death. *Hypertension* **33:** 906–913; 1999.

[34] Galleano, M.; Simontacchi, M.; Puntarulo, S. Nitric oxide and iron: effect of iron overload on nitric oxide production in endotoxemia. *Mol. Aspects Med.* **25:** 141–154; 2004.

[35] Cottart, C. H.; Do, L.; Blanc, M. C.; Vaubourdolle, M.; Descamps, G.; Durand, D., et al. Hepatoprotective effect of endogenous nitric oxide during ischemia–reperfusion in the rat. *Hepatology* **29:**809–813; 1999.

[36] Chen, L.; Wang, Y.; Kairaitis, L. K.; Wang, Y.; Zhang, B. H.; Harris, D. C. Molecular mechanisms by which iron induces nitric oxide synthesis in cultured proximal tubule cells. *Exp. Nephrol.* **9:**198–204; 2001.

[37] Garvey, E. P.; Oplinger, J. A.; Furfine, E. S.; Kiff, R. J.; Laszlo, F.; Whittle, B. J., et al. 1400W is a slow, tight binding, and highly selective inhibitor of inducible nitric-oxide synthase in vitro and in vivo. *J. Biol. Chem.* **272:**4959–4963; 1997.

[38] Jones, S. P.; Bolli, R. The ubiquitous role of nitric oxide in cardioprotection. *J. Mol. Cell. Cardiol.* **40:**16–23; 2006.

[39] Aktan, F. iNOS-mediated nitric oxide production and its regulation. *Life Sci.* **75:** 639–653; 2004.

[40] Li, D.; Hayden, E. Y.; Panda, K.; Stuehr, D. J.; Deng, H.; Rousseau, D. L., et al. Regulation of the monomer–dimer equilibrium in inducible nitric-oxide synthase by nitric oxide. *J. Biol. Chem.* **281:**8197–8204; 2006.

[41] Tummala, M.; Ryzhov, V.; Ravi, K.; Black, S. M. Identification of the cysteine nitrosylation sites in human endothelial nitric oxide synthase. *DNA Cell Biol.* **27:** 25–33; 2008.

[42] Seddon, M.; Looi, Y. H.; Shah, A. M. Oxidative stress and redox signalling in cardiac hypertrophy and heart failure. *Heart* **93:**903–907; 2007.

[43] Kumamoto, T.; Togo, S.; Ishibe, A.; Morioka, D.; Watanabe, K.; Takahashi, T., et al. Role of nitric oxide synthesized by nitric oxide synthase 2 in liver regeneration. *Liver Int.* **28:**865–877; 2008.